IEEE/RSJ International Conference on Intelligent Robotic Systems, October 13-17, 1998, Victoria, B.C., Canada

Position Control of a 3 DOF Piezohydraulic Parallel Micromanipulator

Pasi Kallio*, Quan Zhou*, Mikael Lind**, Heikki N. Koivo**

*Tampere University of Technology, Automation and Control Institute, P.O. Box 692, 33101 Tampere, Finland;
Email: kallio@ae.tut.fi, quan@ae.tut.fi
**Helsinki University of Technology, Control Engineering Laboratory, P.O. Box 3000, 02015TKK, Finland;
Email: mikael.lind@hut.fi, heikki.koivo@hut.fi

Abstract

This paper focuses on the open-loop and closed-loop position control of a tripod-like joint-free parallel micromanipulator that is composed of three piezohydraulic actuation systems. The micromanipulator is controlled in open-loop using a general inverse kinematics model presented earlier for a tripod manipulator having ball and pin joints. Open-loop control is sufficient in many applications but when high accuracy and high speed are required, closed-loop control must be applied. The closed-loop control of the micromanipulator is organized in multiple levels. The first level compensates non-linearities of the actuation systems and the second level controls the position of the end-effector. Level three is a supervisory level and level four tackles automatic operations. Level two, i.e. the position feedback controller, consists essentially of two single input/single output (SISO) proportional-integral (PI) controllers and an incremental form of the inverse kinematics model. The experimental results show that the position feedback control efficiently eliminates drift and vibration of the end-effector.

1 Introduction

Miniaturization has been one of the most important technological trends in the last decades. Microelectronics has paved the way. The sizes of microchips have been reduced from centimeters to micrometers and very high component densities have been achieved. It is expected that microelectromechanical systems will develop in the same way. The successful fabrication and operation of microactuators and micromechanical devices provides the opportunity to produce microminiature machines and mechanical systems. Such systems are called microsystems in Europe, microelectromechanical systems (MEMS) in United States and micromachines in Japan.

Research of microsystems began to gather momentum in 1980's and currently it is one of the most prominent research areas all over the world. Major R&D efforts exist in Japan, United States, many EU countries, South Korea and Taiwan. Evidence of the expectations is also seen in a number of popular articles, such as [10] and [16].

Study of microrobots and micromanipulators is an essential part of microsystems. The structures vary from etched silicon implementations to miniature mechanisms. Nevertheless, the objective of all micromanipulators is to manipulate micrometer sized objects. The size of the micromanipulator is not so important in such applications as biotechnological operations, assembly of microelectromechanical systems, and testing of microelectronics circuits [11]. Small scale manipulators are needed in catheter type of applications, such as medical diagnostics and therapy, for example.

The research of micromanipulation has become more intensive in recent years. Different aspects of micromanipulation have been discussed for example by Arai et. al. [1], Böhringer et. al. [3], Carrozza et. al. [4], Feddema et. al. [5], Goldfarb et. al. [7], Nelson et. al. [20], Pappas et. al. [17] and Sulzman et. al. [19]. Earlier work has been done for example by Arai et. al. [1], Fukuda et. al. [6], Hollis et. al. [8], Hunter et. al. [9] and Sato et. al. [18].

A joint-free parallel micromanipulator is presented in [13]. Its main applications are in biotechnology where needs for *automating* operations have emerged. For example in cell toxicology hundreds of cells are typically injected and therefore an automatic micromanipulator would speed up the process remarkably. Automatic micro-operations can be realized through the integration of advanced control and machine vision methods with a high-performance micromanipulator.

This paper presents open and closed-loop control strategies for the new joint-free parallel micromanipulator. Open-loop control is often sufficient in telemanipulation, since the operator closes the control loop. However, to make automatic micro-operations possible, position feedback control is needed. In this paper, we describe next a piezohydraulic actuation system and its application to the 3 DOF parallel micromanipulator. Section 3 discusses the open-loop control scheme, including an inverse kinematics model of the manipulator. Section 4 focuses on multiple level closed-loop control (non-linearity compensation, position feedback control, supervision and automatic operations). The position feedback control is composed of two single input/single output (SISO)

proportional-integral (PI) controllers and an incremental form of the inverse kinematics. A Hall sensor based measurement system that is used in on-line position control of the micromanipulator is also shortly presented. The paper is concluded in Section 5.

2 Micromanipulator

2.1 Microtelemanipulation

A microtelemanipulator is a device that facilitates remote handling of microscopic objects under computer-assisted human control. The operator obtains visual information about the end-effector and micro objects using a microscope and a CCD camera, as shown in Fig. 1. The micromanipulator is controlled using a joystick.

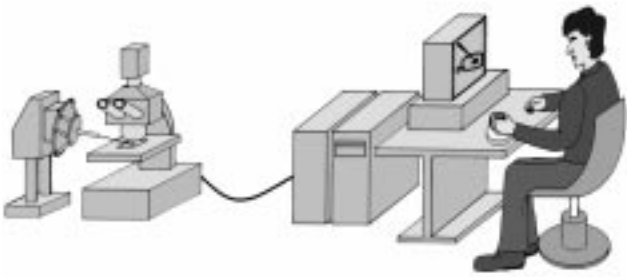

Figure 1: Concept of microtelemanipulation.

2.2 Actuation System

The actuation system consists of a piezoelectric actuator, a small tank and a bellows, as illustrated in Fig. 2. The bellows is a spring type of passive component in which the force required to deform the bellows is directly proportional to the displacement. The piezo actuator is placed in the tank filled with hydraulic oil. When a voltage is applied to the piezo actuator, it deforms. When the actuator buckles, oil flows from the tank to the bellows which elongates. Since the effective area of the bellows is smaller than that of the actuator, the displacement is magnified. The movement range of the actuator is about ± 250 µm. A more detailed description of the actuation system is given in [12].

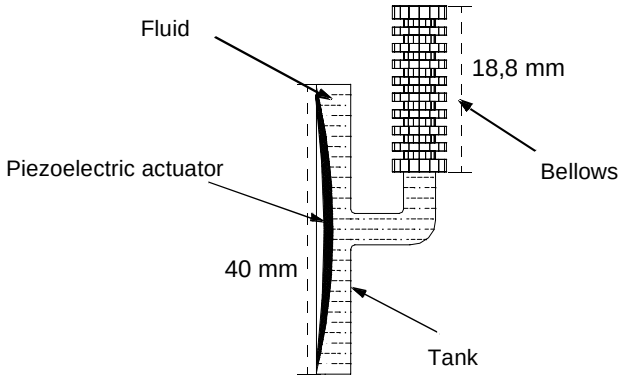

Figure 2: Overview of the actuation system.

2.3 Manipulator Structure

Due to advantages – such as compact size and accuracy – of parallel structures, a parallel configuration was selected for the micromanipulator. The manipulator consists of three identical piezohydraulic actuation systems described in Section 2.2. By connecting them using a mobile platform, a parallel tripod-like configuration illustrated in Fig. 3 is obtained. By changing the lengths of the actuators, the orientation of the mobile platform, and thus the position of the end-effector, can be controlled. The bending character of the bellows results in a joint-free manipulator. The absence of joints simplifies the structure and the manufacturing process.

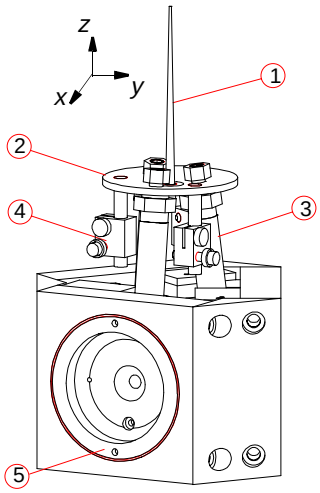

1. End-effector
2. Mobile platform
3. Bellows
4. Pemanent magnets for the Hall sensor measurement
5. Place for the piezo actuator

Figure 3: Overview of the micromanipulator.

Figure 4: Photograph of the micromanipulator.

3 Open-loop Control

In teleoperation open-loop control is typically sufficient, since the operator closes the loop. In applications that are not critical to imperfections (drift

e.g.) of the manipulator, open-loop control can therefore be used to reduce hardware costs.

The structure of the open-loop controller is depicted in Fig. 5. It consists of an inverse kinematics model of the manipulator, rotation, actuator balancing and supervision.

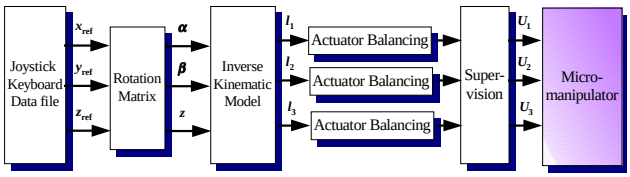

Figure 5: Open-loop control scheme.

Inverse kinematics. The core of the open-loop controller is the inverse kinematics model. Inverse kinematics problem refers to the determination of the link lengths for a given pose of the mobile platform. Lee and Shah [15] have presented inverse and forward kinematics models for a 3 DOF manipulator that has ball joints between the links and the mobile platform and pin joints between the links and the base platform. The mobile platform rotates about the *x* and *y* axes and translates along the *z*-axis (*x*-, *y*- and *z*-axis directions as shown in Fig. 3), i.e. the manipulator has two orientational and one translational degrees of freedom.

The bellows-based joint-free manipulator has been modeled using a similar inverse kinematics model as presented by Lee and Shah. Tests and measurements have proven that the model describes well the inverse kinematics of the bellows-based manipulator. The model is given in Equations (1) - (6), see [15] for more details. When the rotation (α and β) of the mobile platform about the *x* and *y* axes and the translation (z_c) along the *z*-axis are given, the link lengths can be computed using the following equations:

$$\gamma = \operatorname{atan}\left(\frac{\sin\alpha\sin\beta}{\cos\alpha + \cos\beta}\right) \quad (1)$$

$$X_c = \frac{\rho}{2}(n_1 - o_2) \quad (2)$$

$$Y_c = -\rho n_2 \quad (3)$$

$$L_1^2 = (n_1\rho + X_c - 1)^2 + (n_2\rho + Y_c)^2 + (n_3\rho + Z_c)^2 \quad (4)$$

$$\begin{aligned} L_2^2 = \frac{1}{4}\{&(-n_1\rho + \sqrt{3}o_1\rho + 2X_c + 1)^2 \\ &+ (-n_2\rho + \sqrt{3}o_2\rho + 2Y_c - \sqrt{3})^2 \\ &+ (-n_3\rho + \sqrt{3}o_3\rho + 2Z_c)^2\} \end{aligned} \quad (5)$$

$$\begin{aligned} L_3^2 = \frac{1}{4}\{&(-n_1\rho + -\sqrt{3}o_1\rho + 2X_c + 1)^2 \\ &+ (-n_2\rho - \sqrt{3}o_2\rho + 2Y_c + \sqrt{3})^2 \\ &+ (-n_3\rho - \sqrt{3}o_3\rho + 2Z_c)^2\} \end{aligned} \quad (6)$$

where $\rho = \frac{r}{R}$, $L_i = \frac{l_i}{R}, i = 1, 2, 3$, $X_c = \frac{x_c}{R}, Y_c = \frac{y_c}{R}$, $Z_c = \frac{z_c}{R}$, α, β and γ are rotations about the *x*-, *y*- and *z*-axes, respectively, x_c, y_c and z_c are the coordinates of the centre of the mobile platform, *r* and *R* are the radii of the mobile platform and the "base platform", respectively, l_i are the lengths of the actuators and ***n***, ***o*** and ***a*** are the column vectors of the roll-pitch-yaw rotation matrix. The model assumes that the actuators are equally spaced at 120º on both platforms.

Rotation. For intuitive operation, the operator should be able to give the *x*, *y*, *z* coordinates of the end-effector – instead of the orientation of the mobile platform – as reference signals. Therefore, the *x*, *y* and *z* coordinates given by the operator are transformed into corresponding pose (α, β and z_c) of the mobile platform using rotation. The rotated reference signal is used as an input for the inverse kinematics model that generates the link lengths.

Actuator balancing. The three actuation systems never have exactly identical behavior. Therefore, when the same voltage is applied to the actuation systems their displacements are different. To eliminate the difference, the displacements of the actuation systems are balanced using second order polynomials. Furthermore, the voltage - displacement relation of the actuation system is non-linear. This non-linearity has also been taken into account using second order polynomial. An result of the actuator balancing is given in Fig. 6.

Supervision. When the manipulator reaches the limits of the work space, the supervision block warns the operator. If the manipulator is driven, in spite of the warning, to the edge of the workspace the software prevents movements to unfavorable directions and thus prevents the manipulator to be driven into singular conditions.

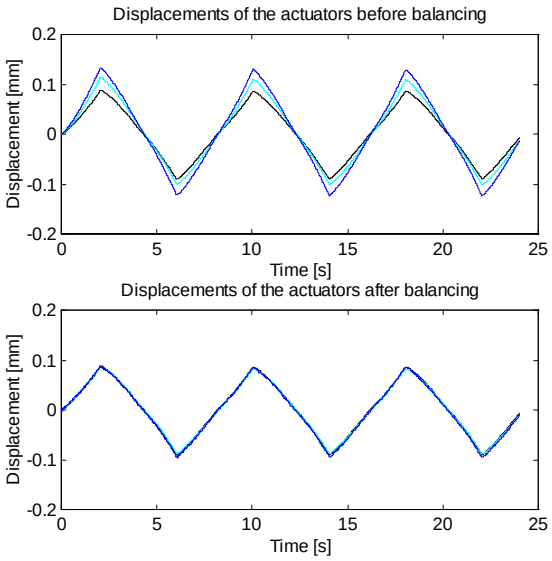

Figure 6: Actuator balancing.

4 Closed-loop Control

In some microtelemanipulation applications, such as patch-clamp measurements where electrical quantities of cell membranes are studied, the end-effector must stay exactly in its position during the operation. Therefore, the drift of the actuators must be eliminated. Moreover, automating micro-operations requires high positioning accuracy and high speed. To fulfill the requirement of high accuracy, drift elimination and high speed, closed-loop control must be applied.

The control of the micromanipulator is organized in multiple levels, as shown in Fig. 7. The first level consists of three local feedback loops that compensate non-linearities of the piezoelectric actuators. The displacement of each piezoelectric actuator is measured using a strain gage. The position of the end-effector is controlled at level 2 using Hall sensors. Level 3 supervises the micromanipulator as described in Section 3. The fourth level will be used to tackle automatic manipulation. It generates the trajectory of the end-effector for example in automatic cell injections. Pattern recognition properties of the vision system can be used to further automate the operation.

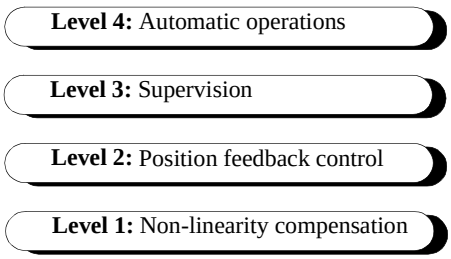

Figure 7: Control levels of the micromanipulator.

Currently levels two and three have been implemented. Level 1 has not yet been applied to the manipulator but it has been tested in a separate actuator. The closed-loop control currently includes PI controllers, rotation of the PI controller outputs, a Jacobian matrix of the manipulator, measurement mapping and supervision control. The structure of the closed-loop controller is presented in Fig. 8.

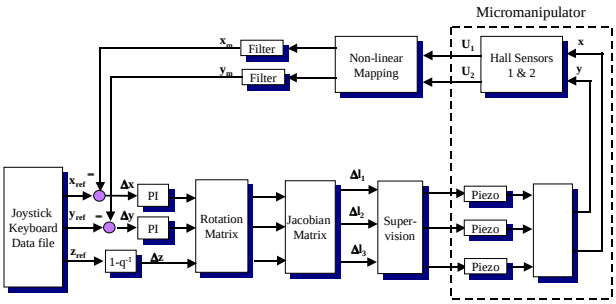

Figure 8: Overview of the closed-loop controller.

Measurement. To realize the position feedback control, the position of the end-effector tip should be measured – either directly or indirectly. The movement of the end-effector is detected using a vision system built at VTT Automation (Technical Research Centre of Finland). The vision system uses a DSP system together with the chamfer matching algorithm to detect the position of the end-effector [14]. However, the vision system cannot be used in *on-line* control as the speed of the vision hardware is currently too slow. The ultimate goal, i.e. to use the vision system in on-line control, requires more powerful hardware.

The orientation of the mobile platform and thus the position of the end-effector are currently measured using Hall sensors. As the Hall sensors do not directly measure the position of the end-effector, the vision system must be used off-line to calibrate the Hall sensor measurement. The vision system measures the movement of the end-effector only at the *xy*-plane and therefore, two Hall sensors are used. The Hall sensors are mounted atop the actuator tanks, and permanent magnets are attached on the mobile platform using movable rods, as presented in Fig. 3.

When the end-effector moves along the *x*-axis, for example, both magnets move with respect to the Hall sensors. Both sensors respond and therefore a mapping must be found between the output voltages of the Hall sensors and the coordinates of the end-effector. The relationship between the Hall sensor signals and the coordinate estimates is presented in Equation (7)

$$\begin{aligned} \hat{x} &= f_1(u_1, u_2) \\ \hat{y} &= f_2(u_1, u_2) \end{aligned} \tag{7}$$

where $\hat{x}$ and $\hat{y}$ are the estimates for the end-effector coordinates, u_1 and u_2 are output voltages of the Hall sensors and f_1 and f_2 are non-linear functions describing the mapping between the Hall sensor signals and the end-effector coordinates.

The mapping has been determined using regression analysis and it has the following form:

$$\begin{bmatrix} \hat{x} \\ \hat{y} \end{bmatrix} = \begin{bmatrix} a_{11} & a_{12} & a_{13} & a_{14} & a_{15} \\ a_{21} & a_{22} & a_{23} & a_{24} & a_{25} \end{bmatrix} \begin{bmatrix} u_1 \\ u_2 \\ u_1 u_2 \\ u_1^2 \\ u_2^2 \end{bmatrix}. \tag{8}$$

Position controller. The position controller consists essentially of two parts: PI controllers and a Jacobian matrix. Since it is difficult to measure the movement of the end-effector along the *z*-axis using the vision system, the Hall sensor measurement cannot be calibrated in 3-D. Therefore, only *x* and *y* coordinates are currently controlled in closed-loop, whereas the *z*-coordinate is open-loop controlled. Two SISO PI controllers are used to

control the position of the end-effector at the *xy*-plane. The change in the reference signal of the *z*-coordinate is, in turn, used for driving the manipulator in the *z*-axis direction.

As discussed in Section 3, the inverse kinematics presents the manipulator with two orientational and one translational (*z*-axis direction) degrees of freedom. As the operator preferably commands the manipulator in translation directions, the reference movements along the *x* and *y* axes must be transformed into rotations. This is done by the rotation block. After rotation, the final control signals for the piezoelectric actuators are computed using the inverse kinematics. A general inverse kinematics model determines the link lengths when the pose of the mobile platform is given. However, in closed-loop control the *pose change* is utilized and therefore an incremental form of the model providing changes in the link lengths for the given pose change is needed, see Equation (9). The incremental inverse kinematics, i.e. the Jacobian matrix, is obtained by differentiating the general inverse kinematics model. Due to the complexity of the model given in Equations (1) – (6), a simpler model was applied. The simplified model assumes that small rotations of the mobile platform correspond the end-effector movement in *x* and *y* axis directions. Simulations show that the model results in decoupled translations of the end-effector. The Jacobian matrix of the manipulator is given in Equation (10).

$$\Delta \boldsymbol{l} = \boldsymbol{J} \Delta \boldsymbol{p} \tag{9}$$

where $\Delta \boldsymbol{p} = \begin{bmatrix} \alpha & \beta & z \end{bmatrix}^T$

$$\boldsymbol{J} = \begin{bmatrix} (\alpha + u_1)/l_1 & (\beta + v_1)/l_1 & z/l_1 \\ (\alpha + u_2)/l_2 & (\beta + v_2)/l_2 & z/l_2 \\ (\alpha + u_3)/l_3 & (\beta + v_3)/l_3 & z/l_3 \end{bmatrix} \tag{10}$$

where $u_i = r\cos\varphi_i - R\cos\theta_i$, $v_i = r\sin\varphi_i - R\sin\theta_i$, $\varphi_1 = 0^o$, $\varphi_2 = 120^o$, $\varphi_3 = -120^o$, $\theta_1 = 0^o$, $\theta_2 = 120^o$, $\theta_3 = -120^o$ and α, β, r, R and l_i are as in Equations (1) – (6).

4.1 Experimental Results

The result of a control experiment that was made to demonstrate the elimination of the drift is presented in Fig. 9. In the experiment, the end-effector was first commanded to move slowly along the *x*-axis, was then hold for five seconds and finally moved back. Although the reference signal was held at a constant value in open loop control, the end-effector moved slightly, because of the drift of piezoelectric actuators. When the position feedback control is introduced, the drift is totally eliminated.

Due to the flexibility of the bellows, the end-effector vibrates easily if the manipulator is moved in large steps or if external mechanical disturbances influence the manipulator. The vibration can be reduced using the position feedback control as illustrated in Fig. 10.

Figure 9: Results of the drift elimination experiment. Reference signal is presented using a dashed line.

The micromanipulator has been demonstrated in the separation of micro particles. The tests have shown that the micromanipulator can easily be used for handling glass spheres whose diameter varies from 10 to 100 micrometers. Based on the experiments, the planar workspace of the manipulator covers 1.5 mm and 0.6 mm in *x*- and *y*-axis directions, respectively. Its maximum vertical displacement along the *z*-axis is about 0.25 millimeters. The displacement resolution of the manipulator is better than one micrometer. The maximum speed of the closed-loop controlled micromanipulator is about 4 mm/s.

Figure 10: Results of the step response experiment.

5 Conclusions

This paper discusses the control of a piezohydraulic parallel micromanipulator. Micromanipulators have several areas of applications, such as biotechnology, assembly of microsystems, microsurgery and testing of microelectronics circuits. Currently in many applications

the operator performs the task using a joystick but in an increasing number of applications automatic operations are required. To implement high speed and high accuracy automatic functions, closed-loop control is needed.

The main contribution of this paper is to present a closed-loop control strategy – being based on two SISO PI controllers and an incremental form of the inverse kinematics model – for a parallel micromanipulator. Furthermore, the paper presents a Hall sensor based measurement method that makes on-line position feedback control of the micromanipulator possible. Finally, the paper shows that an inverse kinematics model that has been presented for a tripod-like parallel manipulator having ball and pin joints between the links and the platforms can be used in the open-loop control of the proposed bellows-based joint-free manipulator.

Acknowledgment

The authors wish to thank the Technology Development Centre of Finland (TEKES) and the Academy of Finland for funding the project. Moreover, we acknowledge the fruitful collaboration with Juha Korpinen and Jouko Viitanen at VTT Automation (Technical Research Centre of Finland) and Hannu Kojola and Markku Ojala at Wallac Oy. We like to thank the Electrical Workshop at TUT for constructing the mechanical parts.

Refereces

[1] Arai, F. & Fukuda, T. “Adhesion-type Micro Endeffector for Micromanipulation”. *Proceedings of the IEEE ICRA’97*, Albuquerque, New Mexico, USA, April 1997, pp. 1472 – 1477.

[2] Arai, T., Larsonneur, R. & Jaya, Y. M. “Calibration and Basic Motion of a Micro Hand Module”. *IEEE IECON’93*, Lahaina, Maui, Hawaii, USA, November 1993.

[3] Bohringer, K.-F., Goldberg, K., Cohn, H., Howe, R. & Pisano, A. “Parallel Microassembly with Electrostatic Force Fields”. *Proceedings of the IEEE ICRA*’98, Leuven, Belgium, May 1998, pp. 1204 – 1211.

[4] Carrozza, M.C., Dario, P., Menciassi, A. & Fenu, A. “Manipulating Biological and Mechanical Micro-Objects Using LIGA-Microfabricated End-Effecters” *Proceedings of the IEEE ICRA*’98, Leuven, Belgium, May 1998, pp. 1811 – 1816.

[5] Feddema, J.T. & Simon, R.W. “CAD-Driven Microassembly and Visual Servoing”. *Proceedings of the IEEE ICRA*’98, Leuven, Belgium, May 1998, pp. 1212 – 1219.

[6] Fukuda, T., Fujiyoshi, M., Arai, F. & Matsuura, H. "Design and Dexterous Control of Micromanipulator with 6 D.O.F.". *Proceedings of the IEEE ICRA*’91, Sacramento, USA, April 1991. pp. 1628 – 1633.

[7] Goldfarb, M. & Speich, J.E. “Design of a Minimum Surface-Effect Three Degree-of-Freedom Micro-manipulator”. *Proceedings of the IEEE ICRA*’97, Albuquerque, New Mexico, USA, April 1997, pp. 1466 – 1471.

[8] Hollis, R., Salcudean, S. & Allan P. “A Six-Degree-of-Freedom Magnetically Levitated Variable Compliance Fine-Motion Wrist”: Design, Modeling, and Control. *IEEE Transactions on Robotics and Automation*. 1991. Vol. 7, no. 3, pp. 320 – 332.

[9] Hunter, I., Lafontaine, S., Nielsen, P., Hunter, P. & Hollerbach, J. “Manipulation and Dynamic Mechanical Testing of Microscopic Objects Using a Tele-Micro-Robot System”. *Proceedings of the IEEE ICRA’89*, Scottsdale, USA, May 1989. 1553 – 1558.

[10] Jaroff, L., “A New Lilliputtian World of Micromachines”, *TIME*, December 2, 1996

[11] Kallio, P. and Koivo, H. N., “Microtelemanipulation: a Survey of the Application Areas”, *Proceedings of the International Conference on Recent Advances in Mechatronics, ICRAM’95*, Istanbul, Turkey, August 1995, pp. 365 – 372.

[12] Kallio, P., Lind, M., Kojola, H., Zhou, Q., Koivo, H., “An Actuation System for Parallel Link Micromanipulators”, *Proceedings of the Intelligent Robots and Systems, IROS'96*, Osaka, Japan, November 1996, pp. 856 – 862.

[13] Kallio, P., Lind, M., Zhou, Q., Koivo, H. “A 3 DOF Piezohydraulic Parallel Micromanipulator”. *Proceedings of the IEEE ICRA’98*, Leuven, Belgium, May 1998.

[14] Korpinen, J., “Micromanipulator Control Using Machine Vision”. *Proceedings of Vision for Control Aspects of Mechatronics, ViCAM'96*, Portugal, September 1996.

[15] Lee, K.-M. & Shah, D. K., “Kinematic Analysis of a Three-Degrees-of-Freedom In-Parallel Actuated Manipulator”. *IEEE Journal of Robotics and Automation*, Vol. 4, No. 3, June 1988, pp. 354 – 360.

[16] New Wave in High-tech: “Tiny Motors, Big Future”, *The New York Times*, January 27, 1997.

[17] Pappas, I & Codourey, A. “3D Visual Control of Microrobots”. *Workshop on Micro Mechatronics and Micro Robotics, IEEE ICRA’98*, Leuven, Belgium, May 1998.

[18] Sato, T., Koyano, K., Nakao, M. & Hatamura, Y. “Novel Manipulator for Micro Object Handling as Interface Between Micro and Human Worlds”. *Proceedings of the 1993 IEEE International Conference on Intelligent Robots and Systems*, Yokohama, Japan, July 1993. pp. 1674 – 1681.

[19] Sulzman, A. “3D Sensor based Microassembly and Quality Control Overview and Examples”. *Workshop on Precision Manipulation at Micro and Nano Scales, IEEE ICRA’98*, Leuven, Belgium, May 1998.

[20] Vikramaditya, B. & Nelson, B. “Visually Guided Microassembly Using Optical Microscopes and Active Vision Techniques”. *Proceedings of the IEEE ICRA’97, Albuquerque*, New Mexico, USA, April 1997, pp. 3172 – 3177.